Journal of Hydrology 664 (2026) 134632

Contents lists available at ScienceDirect

Journal of Hydrology

journal homepage: www.elsevier.com/locate/jhydrol

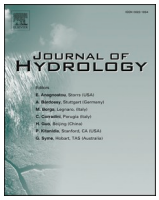

Research papers

Magnitude and impacts of non-rainfall water inputs and nocturnal evapotranspiration on temperate grassland ecosystems

Yafei Li [a,b,1,*], Andreas Riedl [a,1], Nina Buchmann [a], Werner Eugster [a,2]

[a] Department of Environmental Systems Science, ETH Zürich, Zürich 8092, Switzerland
[b] Agroecology and Environment, Agroscope, Zürich 8046, Switzerland

ARTICLE INFO

This manuscript was handled by Amilcare Porporato, Editor-in-Chief, with the assistance of Samantha Hartzell, Associate Editor

Keywords:
Dew
Fog
Water budget
Micro-lysimeter
Environmental drivers
Water-carbon relation

ABSTRACT

Non-rainfall water (NRW, mainly dew and fog) and night-time evapotranspiration (ET_{night}) are opposite phenomena which induce water gain and water loss of ecosystems, respectively. However, how NRW inputs and ET_{night} vary across spatial scales, and what drives their flux magnitude is less clear. In this study, we combined highly accurate micro-lysimeters with environmental measurements to investigate the spatial variability of NRW inputs and ET_{night} at nine grasslands as well as the most important drivers of their flux magnitude. Further, we explored the influence of NRW inputs and ET_{night} on net ecosystem CO_2 exchange in the morning hours. Our results showed that changes in NRW inputs and ET_{night} were independent of elevation, but strongly affected by terrain. Moreover, NRW inputs and ET_{night} were controlled by different environmental drivers, with NRW inputs mainly driven by air temperature changes and event duration, while ET_{night} was mainly driven by dew point depression, soil moisture, and wind speed. Net ecosystem exchange in the early morning hours did not benefit from NRW inputs during the previous night. Our study revealed that the relevance of NRW inputs for temperate grasslands was low, but increasing ET_{night} losses due to climate change will pose additional challenges to grasslands in the future.

1. Introduction

Non-rainfall water (NRW), defined here as dew, fog, hoar frost, and rime, is a potential water source for terrestrial ecosystems. In drylands, dew can occur on more than half of the days of the year, and contribute more than 5 % of annual precipitation (Jia et al., 2019; Yokoyama et al., 2021). In temperate grassland ecosystems, annual NRW inputs were reported to be between 4 and 7 % of total precipitation (Groh et al., 2018; Xiao et al., 2009), which is a rather small amount compared to annual rainfall. However, during rain-free periods, NRW can compensate 20 % of water loss by evapotranspiration, and can thus be an important water source for plants (Li et al., 2021; Munné-Bosch and Alegre, 1999). Plants can benefit from NRW inputs via foliar water uptake, via water vapor exchange with a high-humid atmosphere (Boucher et al., 1995; Dawson and Goldsmith, 2018; Goldsmith, 2013; Limm et al., 2009), and via NRW evaporative cooling (Eugster et al., 2006; Minnis et al., 1997).

While NRW inputs were extensively studied in arid regions (Jacobs et al., 2002; Malek et al., 1999; Ucles et al., 2013), only few studies have focused on NRW in temperate regions (Groh et al., 2018; Jacobs et al., 2006; Xiao et al., 2009). Eddy-covariance methods can reliably quantify ecosystem water vapor fluxes (Baldocchi, 2014), but have large uncertainties to quantify NRW gains due to the occurrence of NRW inputs mostly on nights with a stably-stratified boundary layer (Jacobs et al., 2006). Weighing lysimeters and micro-lysimeters have been widely used hydrometric methods to quantify NRW gains (Agam and Berliner, 2006; Riedl et al., 2022). Due to logistical reasons, many lysimeter-based studies focused on single (Jacobs et al., 2006; Xiao et al., 2009) or two rather similar sites (Groh et al., 2018). However, NRW inputs can be spatially highly variable due to climatic conditions, soil characteristics, vegetation types and thus related canopy structure and phenology, as well as ecosystem management practices (Tomaszkiewicz et al., 2017; Zhang et al., 2009). Thus, quantification of NRW inputs and their spatio-temporal variability in amount and frequency along a spatial gradient is still scarce, limiting the assessment of NRW inputs at regional scales.

While water can be gained during nights via NRW inputs, water can

* Corresponding author at: Agroecology and Environment, Agroscope, Zürich 8046, Switzerland.
E-mail addresses: yafei.li@agroscope.admin.ch, l.yafei@outlook.com (Y. Li).
[1] These authors contributed equally to this work.
[2] Werner Eugster supervised this work until his death, May 2022.

https://doi.org/10.1016/j.jhydrol.2025.134632
Received 30 June 2025; Received in revised form 17 October 2025; Accepted 17 November 2025
Available online 19 November 2025

also be lost due to nocturnal evapotranspiration (ET_{night}). ET_{night} was reported to range from 3.5 to 25 % of daytime evapotranspiration (Caird et al., 2007; Groh et al., 2019; Guo et al., 2023; Padron et al., 2020). Groh et al. (2019) reported that ET_{night} in temperate grasslands was mostly related to evaporation from surfaces. However, other studies showed evidence of nocturnal stomatal opening across many plant species and functional types (Li et al., 2023b; Resco de Dios et al., 2019; Yu et al., 2019), and water loss via nocturnal transpiration of plants. For example, ET_{night} of *Arabidopsis* was shown to equal up to 43 % of its daytime transpiration (Christman et al., 2009). But insights into ET_{night} fluxes at ecosystem scale are limited.

Moreover, effects of NRW inputs or ET_{night} losses on carbon relations in ecosystems, such as temperate grasslands, are not well understood. While NRW inputs clearly induce water gain for an ecosystem, they were reported to also improve the carbon gain of forests during fog by alleviating leaf water deficits (Simonin et al., 2009). On the contrary, ET_{night} caused water loss without any carbon gain (Resco de Dios et al., 2019). However, evaporation of dew water was reported to reduce CO_2 uptake of plants during the day (Gerlein-Safdi et al., 2018b; Misson et al., 2005), but also to induce CO_2 loss in a post-fire marine pine forest (Oliveira et al., 2021). Thus, the influence of NRW inputs on temperate ecosystem carbon budgets are highly variable, maybe also across spatial and elevational gradients.

In this study, we present highly accurate NRW quantifications at central European grassland ecosystems, ranging over wide spatial and elevational gradients. We quantified two opposing processes, i.e., NRW inputs resulting in water gains, and ET_{night} leading to water loss. Focusing on rain-free periods, we studied the ecohydrological effects of both processes on temperate grassland ecosystems, with the specific objectives

(1) to quantify high-temporal resolution NRW inputs and ET_{night} over wide spatial and elevational gradients across Switzerland and the Italian-Swiss border during rain-free periods,
(2) to identify environmental drivers of NRW inputs or ET_{night}, and
(3) to assess the effects of NRW inputs and ET_{night} losses on net ecosystem CO_2 exchange of temperate grasslands.

2. Methods

2.1. Field sites

Measurements of NRW inputs and ET_{night} losses were carried out at nine grassland sites, covering wide spatial and elevational (from 400 to 2000 m a.s.l.) gradients (Fig. S1; Table 1). Eight sites were located in Switzerland (Chamau, CH-Cha; Mettmenstetten, CH-Met; Vordemwald, CH-Vor; Eschikon, CH-Esc; Früebüel. CH-Fru; Loco, CH-Loc; Zernez, CH-Zer; Alp Weissenstein, CH-Aws), and one site at the Italian-Swiss border area (Lichtenberg, IT-Lic). Our study was carried out between May 2019 and December 2020, with varying study durations across sites due to logistical reasons (i.e., time consuming instrument installation) and unavoidable data gaps at remote locations. The grassland site management varied from intensive management with five to six cuts per year (e.g., CH-Cha) to extensive alpine grazing (e.g., CH-Aws). The long-term (1981–2020) average air temperature and annual precipitation during 1981–2020 were derived from the nearby MeteoSwiss stations.

2.2. Nocturnal water balance measurements with micro-lysimeters and ancillary sensors

Each grassland site was equipped with agrometeorological measurements for air temperature (T_{air} in °C), relative humidity (RH in %), and wind speed (U in m s^{-1}) at 2 m a.g.l. Three micro-lysimeters (ML) with ancillary sensors were installed at each site to detect and quantify NRW and ET_{night} events. The methods of soil monolith preparation in the ML systems are described in Riedl et al. (2022). The ML systems with a size of 25 cm diameter × 25 cm depth allowed quantifying ML mass changes with an accuracy of ±0.005 mm and having minor effect on the soil micro-environment (Riedl et al., 2022). Ancillary sensors at each site included a visibility sensor (MiniOFS, Optical sensors Sweden AB, Gothenburg, Sweden) installed at 1 m a.g.l., and a leaf wetness sensor (PHYTOS 31, Meter Group AG, Munich, Germany), complemented by soil temperature and moisture sensors (5TM, Meter Group AG, Munich, Germany) installed in 15 cm soil depth inside and outside each ML. Data were recorded with 1 min resolution. ML mass changes were recorded in g and converted to mm.

Our study focused on rain-free periods only. Leaf wetness and precipitation sensors distinguished NRW events from rainfall periods. Visibility sensors detected fog events when visibility was <1000 m. ML mass changes at each site were calculated as average of three ML systems. Negative ML mass changes over a night represent water loss, and the corresponding nights were defined as nocturnal evapotranspiration (ET_{night}) events. On the contrary, positive ML mass changes over a night represent water gain, and the corresponding periods were defined as NRW events. We note that the duration of an ET_{night} event was the entire night-time period; but when NRW inputs and ET_{night} occurred on the same night, the night-time period with NRW input was excluded from the duration of ET_{night} event. On the other hand, NRW events could be longer than a night-time period when NRW inputs started before sunset and/or lasted after sunrise. Sunset and sunrise times at each site were computed using the Python package “Astral v2.2”.

We differentiated among six types of NRW inputs:

(1, 2) Dew or hoar frost: A dew or hoar frost event was indicated by a net ML mass gain, increased leaf wetness, and no rainfall during a night; the event was defined as dew when air temperature was above 0 °C, otherwise as hoar frost.
(3, 4) Fog or rime: A fog or rime event was indicated by a net ML mass gain, increased leaf wetness, a visibility <1000 m, and no rainfall during a night; the event was defined as fog when air temperature was above 0 °C, otherwise as rime.
Combined dew and fog: Dew and fog intermittently occurred during the same NRW event.

Table 1
Overview of grassland sites: site abbreviations, elevation, latitude and longitude, AND geographical region. Average air temperature and annual precipitation during 1981–2020 were derived from nearby MeteoSwiss stations.

Site	Elevation (m a.s.l.)	Latitude (°N)	Longitude (°E)	Geographical region	Average air temperature (°C)	Annual Precipitation (mm)
CH-Cha	393	47.2102	8.4104	Swiss Plateau	9.6	1013
CH-Met	468	47.2510	8.4618	Swiss Plateau	9.6	1013
CH-Vor	473	47.2688	7.9108	Swiss Plateau	9.3	1113
CH-Esc	550	47.4516	8.6827	Swiss Plateau	9.6	1112
IT-Lic	950	46.6501	10.5631	Southern Alps	7.3	1064
CH-Fru	982	47.1158	8.5378	Pre-Alps	6.6	1556
CH-Loc	1000	46.2109	8.6722	Southern Alps	8.0	1445
CH-Zer	1899	46.6639	10.2311	Alps	1.0	879
CH-Aws	1978	46.5833	9.7904	Alps	3.6	1341

Combined hoar frost and rime: hoar frost and rime intermittently occurred during the same NRW event.

To compare NRW and ET_{night} across all sites, we selected a comparison period (from 28 August 2019 until 1 November 2019) which had simultaneous, high quality data at all sites (only 24-hour data gap on 10/11 September 2019 at CH-Loc site existed). The total evapotranspiration (ET_{total}) during the comparison period was derived from nearby MeteoSwiss stations, whilst ET_{night} was quantified by our ML measurements.

2.3. Eddy covariance measurements of net ecosystem CO_2 exchange (NEE)

To assess the effects of NRW inputs and ET_{night} losses on net ecosystem CO_2 exchange (NEE), we used eddy-covariance (EC) data measured at CH-Cha, CH-Fru, and CH-Aws. The EC setup at CH-Cha consisted of a 3-D sonic anemometer (R3-50, Gill Instruments Ltd., Lymington, UK) and an open-path infrared gas analyser (LI-7500, Li-Cor, Lincoln, USA) installed at 2.4 m a.g.l. (Fuchs et al., 2018). The EC setup at CH-Fru consisted of a 3-D sonic anemometer (R3-50, Gill Instruments Ltd., Lymington, UK) and an open-path infrared gas analyser (LI-7500, Li-Cor, Lincoln, USA) installed at 2.55 m a.g.l. (Rogger et al., 2022). The EC setup at CH-Aws consisted of a 3-D sonic anemometer (HS-50, Gill Instruments Ltd., Lymington, UK) and an enclosed-path infrared gas analyser (LI-7200RS, Li-Cor, Lincoln, USA) installed at 1.3 m a.g.l. (Li et al., 2023a).

EC data were measured at 20 Hz, and processed to 30 min averages using the EddyPro software (Version 7.0.4; LI–COR, 2019), following established community guidelines (Aubinet et al., 2012; Pastorello et al., 2020). To remove EC measurements with insufficient turbulence, u^*-filtering (u^*, friction velocity) of EC fluxes was conducted following the methods described in Feigenwinter et al. (2023). EC data include CO_2 fluxes (in μmol m^{-2} s^{-1}), longwave incoming radiation (LW_{in}), and longwave outgoing radiation (LW_{out}). Vapor pressure deficit (VPD) was quantified from ancillary T_{air} and RH measurements with the Python module "meteolib". Volumetric soil water content (SWC) was measured at 5 cm depth (CH-Cha and CH-Fru: ML2x sensors, Delta-T Devices Ltd., Cambridge, UK; CH-Aws: EC-5, Decagon Devices, Inc., Pullman, WA, USA). NEE was derived from CO_2 fluxes measured with EC technique, with negative values denoting net CO_2 uptake, and positive values denoting net CO_2 emissions. Photosynthetic photon flux density (PPFD in μmol m^{-2} s^{-1}; PARlite, Kipp & Zonen B.V., Delft, The Netherlands) measurement at 1.3 m agl every 10 s was averaged to 30-min intervals.

2.4. Surface and dew-point temperature

Vegetation surface temperature (T_0) was calculated with Eq. (1) using Stefan–Boltzmann's law (Li et al., 2021; Moene and van Dam, 2014) as:

$$T_0 = \sqrt[4]{\frac{LW_{out}}{\varepsilon \bullet \sigma}} - 273.15, \quad (1)$$

where an emissivity (ε) of 0.98 was used for wet leaves (T_0 indexed as T_{0w} during NRW input events) and of 0.96 for dry leaves (T_0 indexed as T_{0d} during ET_{night} events) following López et al. (2012); σ is the Stefan-Boltzmann constant equalling $5.67 \cdot 10^{-8}$ W m^{-2} K^{-1}. Suggested by Moene and van Dam (2014), LW_{out} was corrected with Eq. (2) and calculated as:

$$LW_{out} = LW_{out} - (1 - \varepsilon) \cdot LW_{in}. \quad (2)$$

Dewpoint temperature (T_{dew}) was determined with the Magnus equation (Alduchov and Eskridge, 1996) as:

$$T_{dew} = \frac{243.12 \cdot H}{17.62 - H}, \quad (3)$$

with

$$H = \frac{\log10(RH) - 2}{0.4343} + \frac{17.62 \cdot T_{air}}{243.12 + T_{air}} \quad (4)$$

The temperature difference (ΔT) between T_0 and T_{dew} was then determined with Eq. (5):

$$\Delta T = T_0 - T_{dew} \quad (5)$$

2.5. Environmental drivers of NRW inputs and ET_{night} losses

To investigate the influence of meteorological variables on the amount of NRW inputs and ET_{night} losses, we used three datasets to separately build random forest (RF) regressor models: 1) NRW inputs, 2) ET_{night} losses, and 3) combined NRW–ET_{night} events. RF models can capture non-linear relationships between environmental variables and ML water gains or losses, handle large numbers of input variables without prior variable selection, and assess the importance of environmental variables on ML water gains or losses (Breiman, 2001). RF models were built using the Python module "scikit-learn" (Pedregosa, 2011). Feature importance of environmental variables was simulated by permutation importance to assess the influence levels of environmental variables on ML water gains or losses (Strobl et al., 2007).

The following environmental variables were used as model inputs: ΔT_{air} (changes of air temperature during an event), RH, U, LW_{in}, LW_{out}, SWC, T_{soil}, VPD, visibility, and ΔT. For NRW input events, their duration was used as an additional input variable. At CH-Cha, CH-Fru, and CH-Aws sites, full datasets of these environmental variables were measured, and were thus used as model inputs during the period of April 2019 to December 2020.

All environmental variables were used as event averages as defined in Section 2.2. Event periods with data gaps were excluded. Variables were standardized using "StandardScaler "(removing the mean and scaling to unit variance) in the Python module "scikit-learn" (Pedregosa, 2011). Model performance was quantified by the values of R^2 and root mean squared errors (RMSE). Higher R^2 and lower RMSE indicated better performance of models.

2.6. Statistical analysis

A pairwise *t*-test was used to compare NEE during the daytime period after individual NRW input events and ET_{night} nights among the three EC sites CH-Cha, CH-Fru and CH-Aws during the vegetation period (May until September) in 2019 and 2020. The relationships of NEE with T_{air} and PPFD were assessed by ordinary least square regressions. Statistical tests were performed using the Python package "statsmodels" (Seabold and Perktold, 2010).

3. Results

3.1. Determination of non-rainfall water (NRW) inputs and nocturnal evapotranspiration (ET_{night}) losses with micro-lysimeters (ML)

Using MLs, grassland water inputs and losses during rain-free periods were quantified during the course of our study. The increase in ML mass due to water gain, for example, during a night, was used to quantify NRW inputs (Fig. 1). On the contrary, decreasing ML mass indicated water loss and thus ET_{night} losses. During an observation period at the CH-Aws site from 12 September 12:00 to 18 September 12:00 in 2019, three ET_{night} events followed by three NRW input events were observed, based on ML mass changes. During the three ET_{night} events, water loss varied between 0.2 and 0.32 mm per event, while during the three subsequent NRW input events, water gain varied from 0.04 mm to 0.23 mm per event. During this period, diel water loss was larger than the water gain by NRW inputs, hence the final ML mass decreased

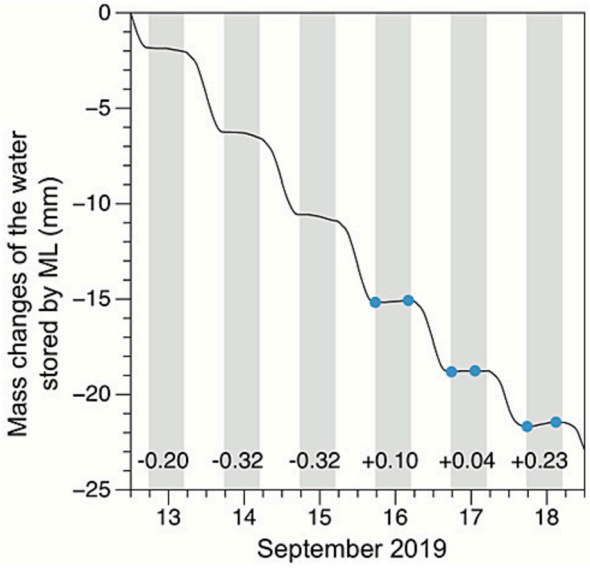

Fig. 1. An example of mass changes of the water stored by a micro-lysimeter (ML) system over a period from 12 September 12:00 to 18 September 12:00 in the year 2019 at CH-Aws site. ML mass changes were averaged over three ML systems. The grey shaded periods indicate night-time. Negative changes in water mass indicatenet water loss due to evapotranspiration, while positive changes indicate net water gain by non-rainfall water (NRW) input events. The duration of an ET_{night} event equals to the night-time period (grey shaded periods); blue dots indicate the start and the end of a NRW input event. (For interpretation of the references to colour in this figure legend, the reader is referred to the web version of this article.)

substantially compared to the beginning of this period.

However, NRW inputs and ET_{night} losses did also take place successively in a single night (Fig. 2). During the night 22/23 May 2019 at CH-Fru, water evaporated until about midnight, as long as the meteorological conditions were conducive to ET_{night} (Fig. S2). From midnight onwards, when meteorological conditions changed to be conducive to NRW inputs, the grassland gained water. Switching from ET_{night} to NRW input reduced the overall grassland water loss, but a net water loss of 0.05 mm was measured from sunset until the termination of NRW input early in the morning.

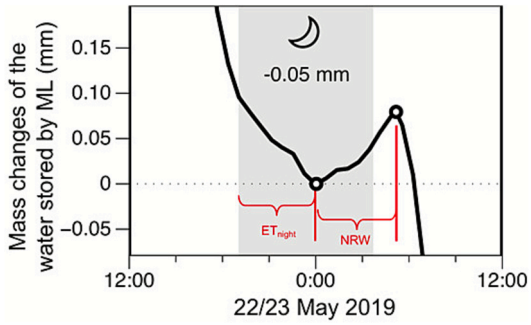

Fig. 2. An example of a night (22/23 May 2019, at CH-Fru site) when nocturnal evapotranspiration (i.e., net water loss, ET_{night}) and non-rainfall water (NRW) input (i.e., net water gain) occurred successively. Water evaporated until midnight, followed by NRW input, before ET started again during the next day. The grey shaded period indicates night-time. Circles indicate the start and the end of the NRW input period. The amount of water changes during this combined ET_{night} and NRW input event is given in mm.

3.2. Amounts and occurrence of non-rainfall water (NRW) inputs and nocturnal evapotranspiration (ET_{night})

Amounts and occurrences of NRW input and ET_{night} events varied among the nine sites, with NRW input events dominanting at the sites CH-Cha, CH-Vor, CH-Esc, CH-Fru, and CH-Aer, but ET_{night} events dominanting at the sites CH-Met, IT-Lic, CH-Loc, and CH-Aws (Fig. 3). Based on 917 measured NRW events, NRW water gains were on average 0.14 ± 0.10 mm $event^{-1}$ and ranged up to 0.70 mm $event^{-1}$ (Fig. 3; Table S1). NRW input events persisted for 0.5 to 18.1 h, with an average duration of around 9 h $event^{-1}$. There was no clear seasonal pattern for the occurrence of NRW inputs. Correspondingly, based on 966 measured ET_{night} events, nocturnal water loss by ET_{night} was on average 0.24 ± 0.16 mm $night^{-1}$, and ranged from 0.0003 to 2.28 mm $night^{-1}$ (Fig. 3; Table S2). Due to the seasonal variability of nocturnal periods, the duration of ET_{night} events varied from 8.1 to 15.6 h $event^{-1}$.

To compare NRW inputs across all sites, we selected a comparison period from 28 August 2019 until 1 November 2019 (grey shaded periods in Fig. 3), with simultaneous and high-quality data for all sites at different elevation, temperature and precipitation conditions (Fig. 4a, b, c). During this comparison period, total NRW gains were up to 6.98 mm at CH-Esc, but as low as 0.12 mm at IT-Lic (Fig. 4d). Furthermore, most NRW input events were observed at CH-Esc, on 45 % of all days, persisting for 4.5–13.6 h $event^{-1}$ (Fig. 4e, f). Least NRW input events occurred at IT-Lic, on 8 % of days lasting for 1.9–6.8 h $event^{-1}$. During this comparison period, the highest NRW gains per event were observed at CH-Zer, with 0.64 mm during a hoar frost event occurring on 13/14 September 2019. Across all sites, average NRW input ranged from 0.02 to 0.33 mm $event^{-1}$ (Fig. 4g). Among the different types of NRW events, dew most frequently occurred at all sites, except for CH-Cha and CH-Vor, where combined dew and fog were the most common NRW events (Fig. 4e). NRW amounts ranged from 0.1 % at CH-Loc to 3.0 % at CH-Esc of the total rainfall during the comparison period (Fig. 4h).

Moreover, during the comparison period, cumulative ET_{night} was up to 13.39 mm at IT-Lic, but only 0.09 mm at CH-Cha (Fig. 4d). ET_{night} occurred on 58 % of all days at IT-Lic, with durations of 10.5–13.8 h $event^{-1}$, but on only 3 % of all days at CH-Zer and CH-Vor, with durations of 10.4–11.2 h $event^{-1}$ (Fig. 4e, f). Most water loss per event occurred at CH-Aws during the night of 21/22 October 2019, with 1.24 mm $event^{-1}$ (Fig. 4g). Across all sites, average ET_{night} water loss ranged from 0.01 to 0.95 mm $event^{-1}$ (Fig. 4g). ET_{night} lost 0.04 % at CH-Cha but 15.2 % at IT-Lic of total rainfall during the comparison period (Fig. 4h). Thus, ET_{night} contributed 0.1 % to 11.6 % of ET_{total} during the comparison period, with highest contribution at IT-Lic but lowest contribution at CH-Cha (Table 2).

Occurrences of ET_{night} (on average, 24 % of all days) were as frequent as those of NRW input events (on average, 25 % of all days) during the comparison period (Fig. 4e). However, the average water loss during ET_{night} events (0.3 mm $event^{-1}$) was four times the average water gain of NRW input events (0.07 mm $event^{-1}$). At four out of nine sites (CH-Aws, CH-Loc, CH-Met and IT-Lic), the total water gain by NRW inputs was on average lower than the water loss during ET_{night} periods (Fig. 4d). However, at the other five sites (CH-Cha, CH-Esc, CH-Fru, CH-Vor and CH-Zer), the opposite pattern was observed.

3.3. Elevational and spatial variability of non-rainfall water (NRW) inputs and nocturnal evapotranspiration (ET_{night})

The cumulative NRW gain was independent of elevation (Fig. 5a), and showed no clear spatial pattern during the comparison period (Fig. 5b). However, cumulative NRW inputs were strongly affected by geographical variations (Fig. 5b). Compared to the total amount of NRW gain on the Swiss plateau (CH-Met, CH-Mor, CH-Cha, and CH-Esc), the amount of NRW gain in the Southern Alps (IT-Lic and CH-Loc) was much smaller, but at similar levels as in the Alps (CH-Aws and CH-Zer). Cumulative ET_{night} loss was also independent of elevation (Fig. 5c), but

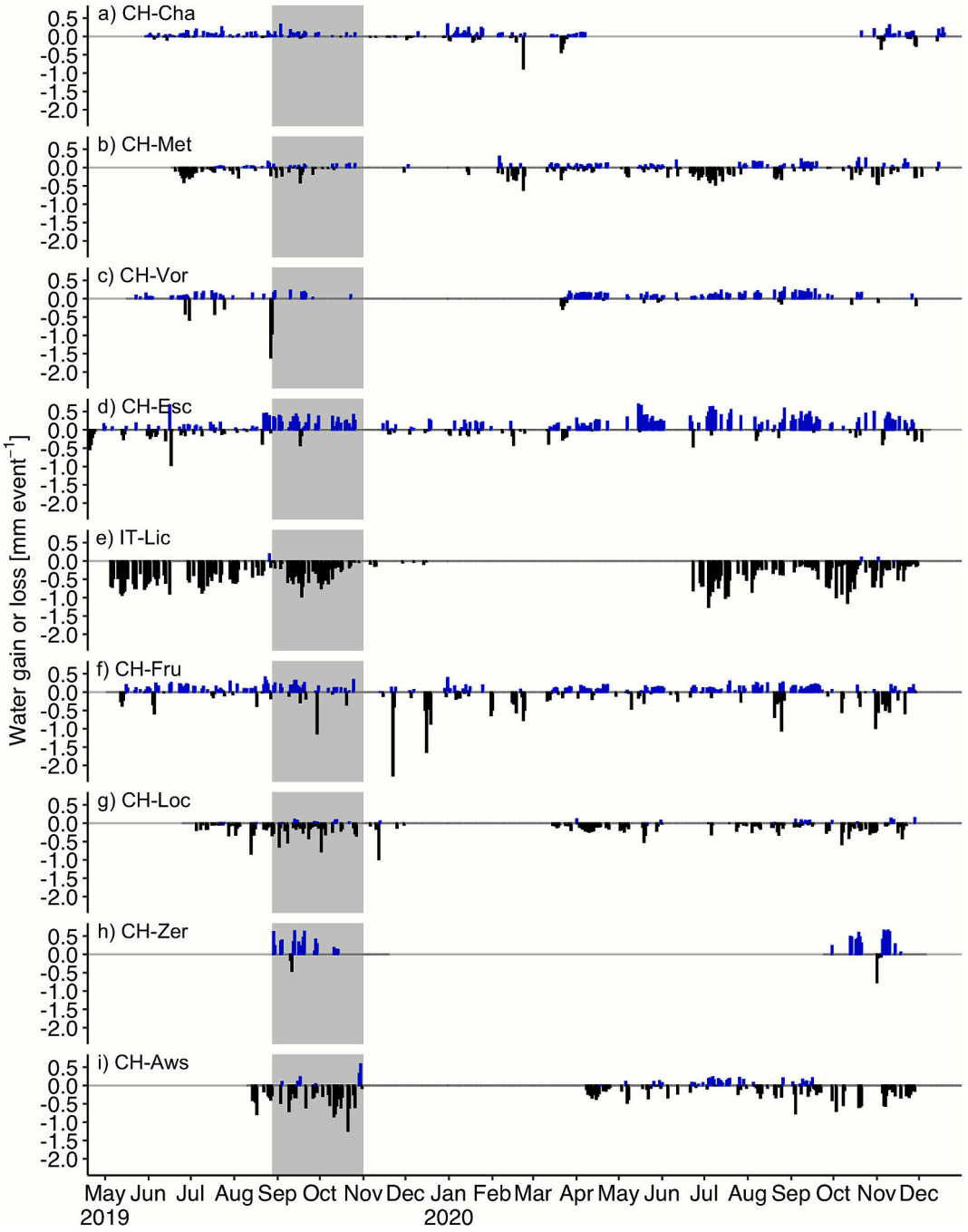

Fig. 3. Non-rainfall water (NRW) inputs and nocturnal evapotranspiration (ET_{night}) at nine sites during the observation period from May 2019 until December 2020. Positive values indicate water gain by NRW inputs (blue), and negative values indicate water loss by ET_{night} (black). Observation periods varied among sites due to logistical reasons and data gaps. The grey shaded area indicates the comparison period with simultaneous and high-quality data at all sites, used for comparing NRW and ET_{night} events. (For interpretation of the references to colour in this figure legend, the reader is referred to the web version of this article.)

tended to be higher in alpine regions (IT-Lic and CH-Loc in the Southern Alps; CH-Aws in Alps; Fig. 5d).

Across the comparison period, regions with more NRW events had generally higher cumulative NRW input amounts ($p < 0.05$; Fig. 6a); similarly, regions with more ET_{night} events had generally higher cumulative ET_{night} losses ($p < 0.001$; Fig. 6b). The amount of cumulative ET_{night} losses tended to be slightly higher at sites with smaller amounts of cumulative NRW inputs (statistically insignificant, $p > 0.05$; Fig. 6c). Correspondingly, regions with more frequent NRW events tended to have lower chance of ET_{night} occurrence (statistically insignificant, $p > 0.05$; Fig. 6d).

3.4. *Influence of environmental drivers on non-rainfall water (NRW) inputs and nocturnal evapotranspiration (ET_{night})*

Compared to ET_{night} occurrences, the periods of NRW input occurred under conditions with larger air temperature changes (ΔT_{air}), higher RH, and thus lower VPD values, weaker wind, negative ΔT (i.e., $T_0 < T_{dew}$) and higher SWC (Table 3). NRW inputs with conditions of <1000 m visibility were due to fog occurrence (Table 3).

Using combined NRW–ET_{night} event data, the RF model ($R^2 = 0.95$; RMSE = 0.04; Fig. S3) delivered better results to model NRW gains and ET_{night} losses than the linear-mixed model ($R^2 = 0.63$; RMSE = 0.11;

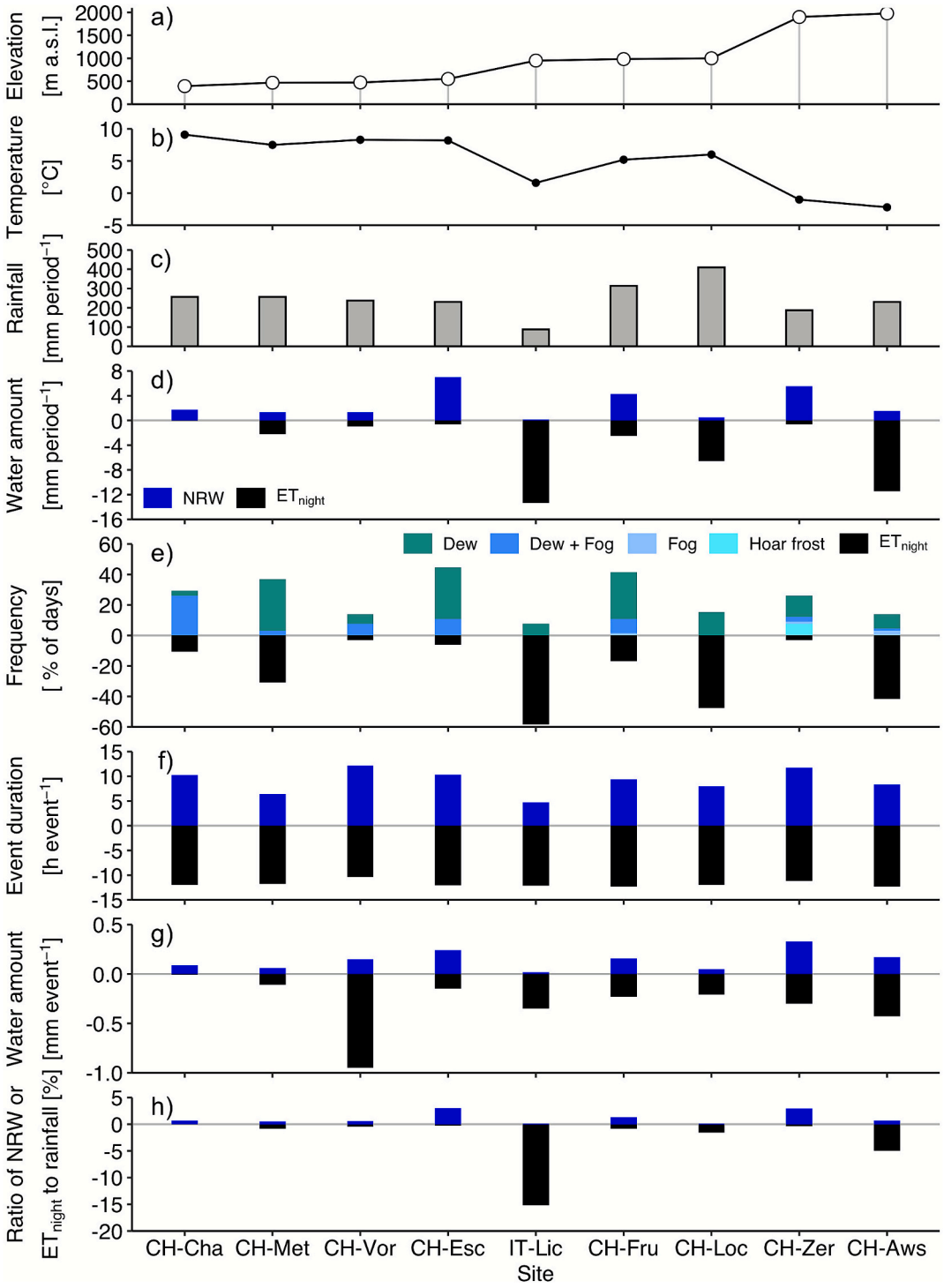

Fig. 4. Environmental conditions and non-rainfall water (NRW) inputs and night-time evapotranspiration (ET_{night}) at nine sites during the comparison period from 28 of August 2019 until 1 November 2019. Positive values (blue) indicate NRW inputs, negative values (black) indicate ET_{night}. a) Elevation. b) Average air temperature, c) Total rainfall. d) Total water gain by NRW inputs and water loss by ET_{night}. e) Occurrence frequency of different NRW events (i.e, dew, dew & fog, fog, hoar frost) and ET_{night} events. f) Average duration of NRW input events and ET_{night} events. g) Average water amount gained per event by NRW inputs and lost by ET_{night}. h) Ratio of total NRW amounts and ET_{night} amounts to total rainfall. (For interpretation of the references to colour in this figure legend, the reader is referred to the web version of this article.)

Fig. S3). Therefore, we used RF models to simulate the relative importance of variables on ML mass changes during NRW input, ET_{night} and combined NRW–ET_{night} events. More than 87 % of the events could be explained with RF models (Fig. 7). The variable importance in the RF regressor models differed by event type, indicating different environmental drivers that affected the occurrence of NRW inputs, ET_{night} and combined NRW–ET_{night} (Fig. 7). The most important drivers of NRW gain were ΔT_{air}, followed by NRW duration, while U, ΔT, LW_{out}, SWC, T_{soil}, VPD, visibility, RH and LW_{in} were less important (Fig. 7a). In contrast, the most important variables for ET_{night} water loss were ΔT, SWC and U, followed by less important variables visibility, RH, LW_{out}, VPD, ΔT_{air}, T_{soil} and LW_{in} (Fig. 7b). Similarly, for combined

Table 2
Night-time evapotranspiration (ET_{night}) and total evapotranspiration (ET_{total}) at nine sites during the comparison period from 28 August 2019 until 1 November 2019. The total evapotranspiration (ET_{total}) during the comparison period was derived from the nearby MeteoSwiss stations, and ET_{night} was quantified by our micro-lysimeter (ML) measurements.

Site	Geographical region	Elevation (m a.s.l.)	ET_{night} (mm)	ET_{total} (mm)	ET_{night}/ET_{total} (%)
CH-Cha	Swiss Plateau	393	0.09	113	0.1
CH-Met	Swiss Plateau	468	2.20	113	1.9
CH-Vor	Swiss Plateau	473	0.95	116	0.8
CH-Esc	Swiss Plateau	550	0.60	120	0.5
IT-Lic	Southern Alps	950	13.39	115	11.6
CH-Fru	Pre-Alps	982	2.53	110	2.3
CH-Loc	Southern Alps	1000	6.55	127	5.2
CH-Zer	Alps	1899	0.61	108	0.6
CH-Aws	Alps	1978	11.49	110	10.4

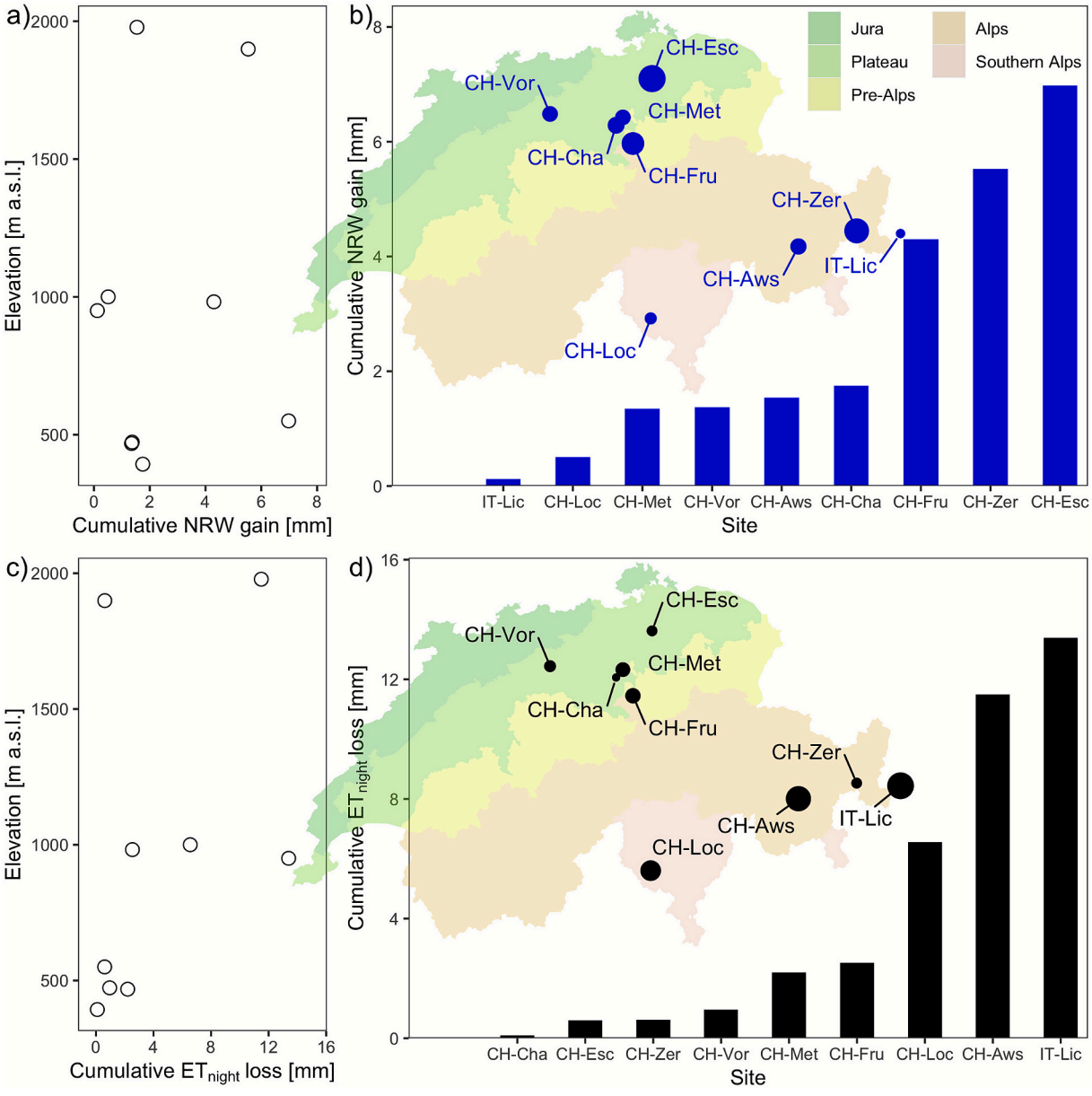

Fig. 5. Spatial variations of cumulative non-rainfall water (NRW) gains and cumulative nocturnal evapotranspiration (ET_{night}) losses at nine sites during the comparison period from 28 August 2019 until 1 November 2019. a) Cumulative NRW gain along an elevation gradient. b) Spatial distribution of cumulative NRW input gain indicated in dot sizes and histogram heights; c) Cumulative ET_{night} loss along an elevational gradient. d) Spatial distribution of cumulative ET_{night} loss indicated in dot sizes and histogram heights. Base map on panels b) and d) was extracted from Swisstopo.

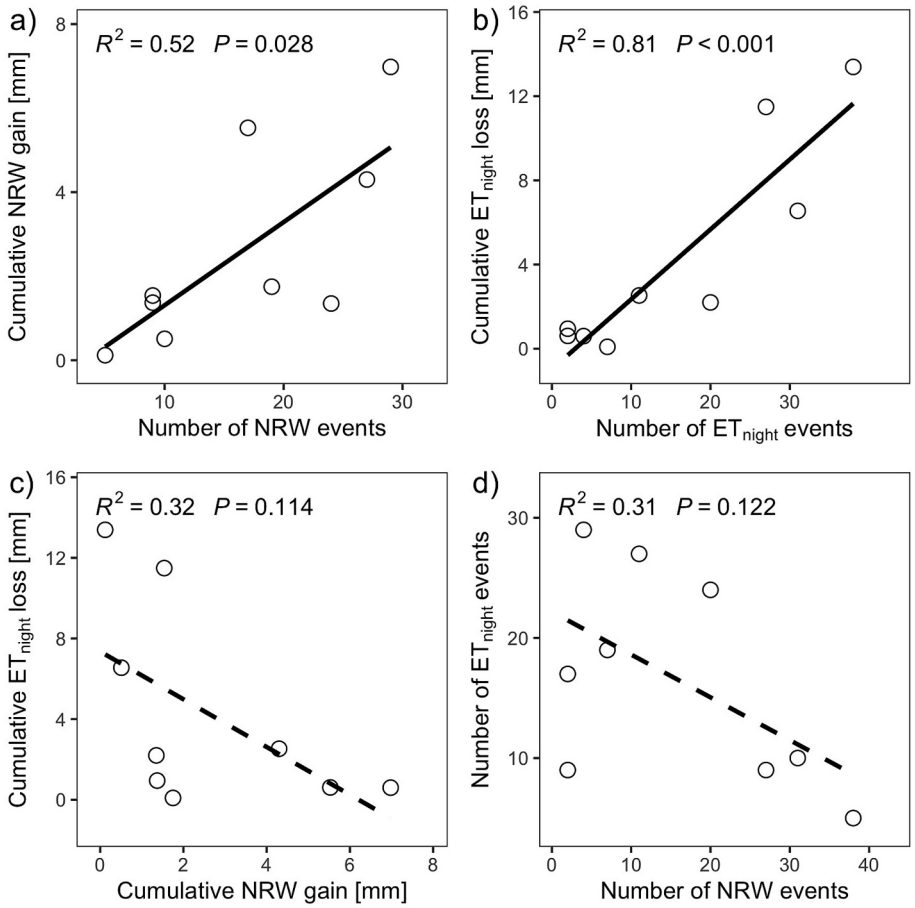

Fig. 6. Relationships of cumulative non-rainfall water (NRW) gain and nocturnal evapotranspiration (ET_{night}) loss with number of events at nine sites during the comparison period from 28 August 2019 until 1 November 2019. a) Cumulative NRW gain vs. number of NRW events. b) Cumulative ET_{night} loss vs. number of ET_{night} events. c) Cumulative NRW gain vs. cumulative ET_{night} loss. d) Number of NRW events vs. number of ET_{night} events.

Table 3
Environmental conditions during the occurrence of non-rainfall water (NRW) inputs and nocturnal evapotranspiration (ET_{night}) at CH-Aws, CH-Cha and CH-Fru during the entire study period from April 2019 until December 2020. Mean ± standard error is given. ΔT_{air}, changes of air temperature during an event; T_{soil}, soil temperature at 5 cm depth; ΔT (= $T_0 - T_{dew}$), temperature difference between vegetation surface temperature (T_0) and the dewpoint temperature of atmospheric air (T_{dew}); RH, relative humidity; VPD, vapour pressure deficit; LW_{in}, longwave-incoming radiation; LW_{out}, longwave-outgoing radiation; U, horizontal windspeed; SWC, volumetric soil water content at 5 cm depth; horizontal visibility < 1000 m indicating fog occurrence;. "n.a." not applicable.

	NRW input	ET_{night}	Difference of NRW and ET_{night}
ΔT_{air} (°C)	5.5 ± 0.3	4.2 ± 0.2	1.3 ± 0.1
T_{soil} (°C)	12.4 ± 0.4	10.4 ± 0.4	2.0 ± 0.0
ΔT (°C)	−1.3 ± 0.1	2.3 ± 0.2	−3.6 ± 0.1
RH (%)	88 ± 1	72 ± 1	16 ± 1
VPD (hPa)	1.95 ± 0.12	3.47 ± 0.19	1.53 ± 0.06
LW_{in} (W m^{-2})	298 ± 2	292 ± 3	7 ± 1
LW_{out} (W m^{-2})	344 ± 2	340 ± 2	5 ± 0
U (m s^{-1})	0.74 ± 0.03	1.50 ± 0.10	−0.76 ± 0.07
SWC (m^3 m^{-3})	0.42 ± 0.01	0.39 ± 0.01	0.03 ± 0.00
Visibility <1000 m (m)	597 ± 41	n.a.	n.a.

NRW–ET_{night} events, the most important variables were ΔT, SWC and RH, followed by less important variables U, ΔT_{air}, visiblity, VPD, T_{soil}, LW_{out} and LW_{in} (Fig. 7c).

3.5. *Effects of non-rainfall water (NRW) inputs and nocturnal evapotranspiration (ET_{night}) on net ecosystem CO_2 exchange (NEE)*

During nights following NRW inputs (143 events) or ET_{night} nights (87 events), grassland NEE within the first two hours after sunrise showed significant differences between these two conditions (*t*-test; $p < 0.01$ within one hour after sunrise; $p < 0.05$ within two hours after sunrise) (Fig. 8a). Beyond these two hours after sunrise, no significant differences between daytime NEE after NRW inputs and NEE after ET_{night} nights were found until 12 h after sunrise (Fig. 8a). Within the first hour after sunrise, NEE after NRW input was lower by 4.75 μmol m^{-2} s^{-1} compared to that after ET_{night} nights, within the first two hours after sunrise by 3.17 μmol m^{-2} s^{-1}, indicating lower net ecosystem CO_2 losses in the early morning hours after NRW inputs. Focussing on daytime NEE within two hours after sunrise following NRW input or ET_{night} nights showed no strong relationship of NEE with T_{air}. However, when NEE were binned into eight bins of equal widths with 2 °C intervals of T_{air}, a clear trend emerged (Fig. 8b). Daytime NEE within two hours after ET_{night} nights increased with temperature (Fig. 8b; $R^2 = 0.48$; $p < 0.05$), indicating higher net ecosystem CO_2 losses, while daytime NEE within two hours after NRW input events showed no clear relationship with T_{air} (Fig. 8b; $R^2 = 0.03$, $p > 0.1$). Under the same T_{air} conditions, NEE after ET_{night} nights tended to be higher than NEE after NRW input nights (Fig. 8b), representing higher net ecosystem CO_2 losses. In contrast,

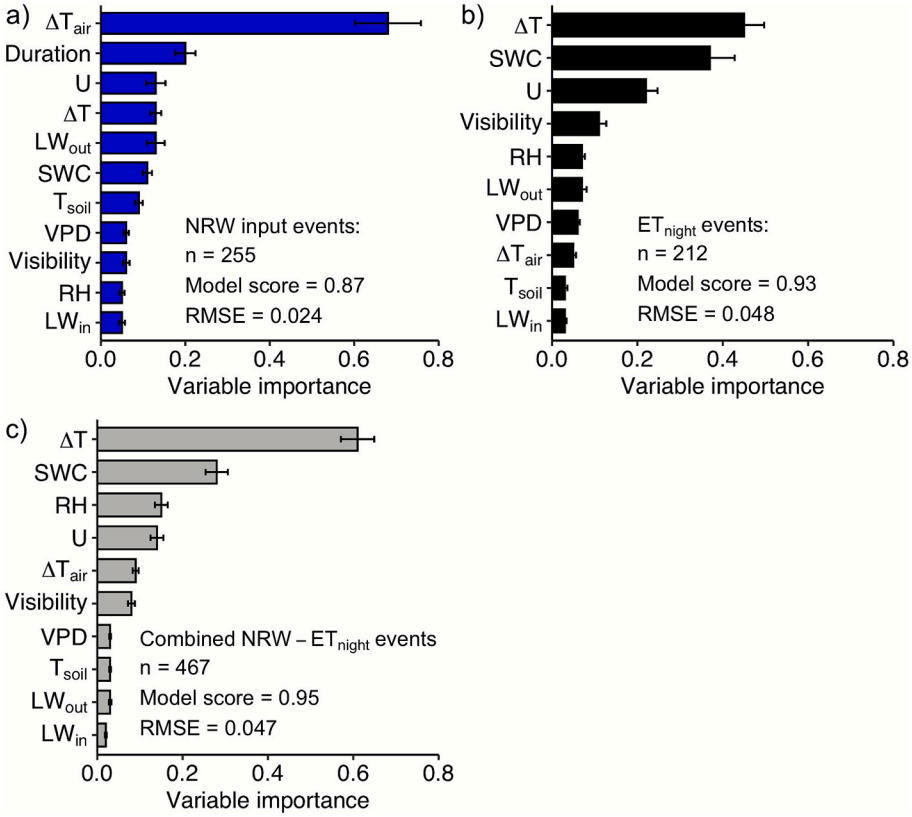

Fig. 7. Importance of environmental variables based on random forest (RF) regressor models for a) non-rainfall water (NRW) inputs, b) nocturnal evapotranspiration (ET_{night}), and c) combined NRW–ET_{night} events during the study period from April 2019 until December 2020 at CH-Aws, CH-Cha, and CH-Fru sites. Input variables include longwave-incoming radiation (LW_{in}, W m^{-2}), longwave-outgoing radiation (LW_{out}, W m^{-2}), relative humidity (RH, %), volumetric soil water content at 5 cm depth (SWC, m^3 m^{-3}), changes of air temperature during an event (ΔT_{air}, °C), the temperature difference between vegetation surface temperature and the dewpoint temperature of the air (ΔT, °C), soil temperature at 5 cm depth (T_{soil}, °C), horizontal wind speed (U, m s^{-1}), horizontal visibility (Visibility, m), and vapor pressure deficit (VPD, hPa). For models of NRW input events (a) duration was also used as an input variable. Total number of events (n), model score, and root mean squared error (RMSE) of RF models are given.

daytime NEE within two hours after sunrise following NRW input or ET_{night} nights was not related to PFFD (Fig. 8c), even when NEE was binned into eight bins of equal widths with 10 μmol m^{-2} s^{-1} interval of PPFD.

4. Discussion

4.1. NRW inputs and ET_{night} losses varied substantially at local and regional scales

For our comparison, we chose the period from 28 August 2019 until 1 November 2019 falls within the growing season, and coincides with a period of relatively low precipitation (see Fig. S4a for monthly precipitation at CH-Cha site). Although our observations cover only two months, they fall within a period when NRW is likely to have high ecological significance.

Overall, the gain and occurrence of NRW inputs in this study were slightly lower than previously reported for European temperate grasslands (Groh et al., 2018; Jacobs et al., 2006), most likely due to the years of our study, two of the warmest and driest years on record (MeteoSwiss, 2025). Groh et al. (2018) reported that dew gains were 1.6–16.3 % of monthly precipitation in Austrian and German grasslands, which was higher than our observation that NRW yields were 0.1–3.0 % of rainfall during the comparison period (Fig. 4h). Jacobs et al. (2006) found that dew occurred on 70 % of nights in a year in a Dutch grassland, which was also higher than our observation with a NRW occurrence on 8–45 % of days during the comparison period (Fig. 4e). Lower NRW gain and occurrence frequency in our study could be due to the very dry conditions during 2019 in Europe compared to humid years in 2004 for Jacobs et al. (2006) and 2014 for Groh et al. (2018) (Fig. S4b; Boergens et al. (2020). However, focusing on the event scale, up to 0.7 mm $event^{-1}$ of dew gain in this study was in line with studies in semi-arid (Aguirre-Gutiérrez et al., 2019) and temperate grasslands (Groh et al., 2018).

Previous studies showed variations in NRW inputs across larger spatial scales, i.e., dry, temperate and tropical grasslands (Aguirre-Gutiérrez et al., 2019; Jacobs et al., 2006; Ritter et al., 2019). In our study, NRW inputs varied across local and regional scales, probably due to geographical variations in the complex terrain in our study area that can induce different local-scale circulations (Stoll et al., 2013). However, NRW inputs were independent of elevation (Fig. 5a). For instance, IT-Lic and CH-Fru sites were located at similar elevations, but much higher ET_{night} water loss than NRW gain was observed at IT-Lic than at CH-Fru (13.39 mm $period^{-1}$ vs. 0.12 mm $period^{-1}$, respectively; Fig. 4d), maybe due to IT-Lic being located on a slope where moisture can be advected downward to the valley bottom instead of contributing to NRW gain (Whiteman et al., 2007). On the contrary, at CH-Fru, higher NRW gain than ET_{night} water loss (4.30 mm $period^{-1}$ vs. 2.53 mm $period^{-1}$, respectively) could profit from the location on a mountain plateau in the Swiss Pre-Alps (Fatichi et al., 2014; Riedl et al., 2022), conducive to moisture accumulation and thus frequent occurrences of NRW inputs (Scherrer and Appenzeller, 2014). Moreover, CH-Cha and CH-Met, two sites located on the Swiss Plateau, were only 6 km away from each other, and had similar total dew gains during the comparison period (1.35–1.75 mm; Fig. 4d). However, compared to CH-Met with dew as the dominant NRW type (Fig. 4e), at CH-Cha fog or combined dew and fog

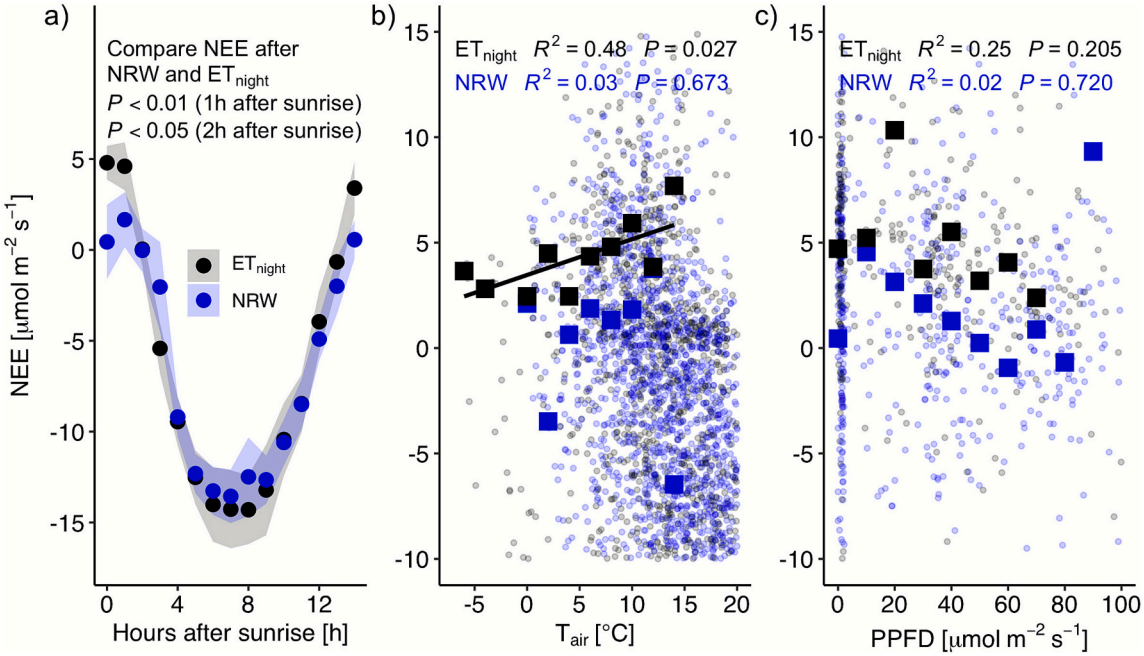

Fig. 8. Relationships of non-rainfall water (NRW) inputs and nocturnal evapotranspiration (ET_{night}) with net ecosystem exchange (NEE), air temperature (T_{air}), and photosynthetic photon flux density (PPFD) based on data from CH-Aws, CH-Cha, CH-Fru during the vegetation period (May until September) in 2019 and 2020: a) NEE vs. time after sunrise, following NRW inputs or ET_{night} nights; symbols indicate hourly averages; shaded areas (blue or grey) indicate 95 % confidence intervals. Significant differences between NEE after NRW and ET_{night} nights are given with $p < 0.05$ and $p < 0.01$ representing the daytime NEE within two hours and one hour after sunrise, respectively. b) Relationship between T_{air} and NEE within two hours after sunrise, following NRW inputs or ET_{night}; dots represent individual data points, and squares show the averages of data bins. Regression coefficients and p-value of regression analyses are given. c) Relationship between PPFD and NEE within two hours after sunrise, following NRW inputs or ET_{night} nights; dots represent individual data points, and squares show the averages of data bins. Regression coefficients and p-value of regression analyses are given. (For interpretation of the references to colour in this figure legend, the reader is referred to the web version of this article.)

conditions occurred more frequently, maybe due to its location at a broad valley bottom where cold air drainage contributes to the moisture supply of fog development under saturated conditions (Eugster and Siegrist, 2000; Li et al., 2021).

ET_{night} losses were highly variable across space as well (Fig. 5d), with higher ET_{night} at three of the four sites in the alpine region compared to sites in lower-elevation regions, probably due to the generally stronger turbulence in the alpine region. ET_{night} was independent of elevation (Fig. 5c) for grassland ecosystems in our study, which corresponds to the results by Allan et al. (2021) for Australian savannas, despite a smaller elevation gradient in their research compared to this study. Sites with high ET_{night} losses seemed to have low NRW inputs and vice versa (Fig. 6c). Existing studies reported varying ET_{night}/ET_{total} ratios, with 6.3 % globally (Padron et al., 2020), 4.9–11.1 % in Australian savannas (Han et al., 2021), and 3.3–9.0 % in German grasslands (Groh et al., 2019). However, our data based on ML measurements showed larger variability in ET_{night}/ET_{total} ranging from 0.1 % to 11.6 % (Table 2), which corresponded to 1.7–14 % found in alfalfa growing cycles (Malek, 1992). The spatial heterogeneity might cause the large variability of ET_{night}/ET_{total}, which could be further induced by uncertainties of using eddy-covariance and hydrometric approaches to quantify ET_{night} (Jacobs et al., 2006).

ET_{night} in temperate grasslands was found to be mostly related to evaporation (Groh et al., 2019), but some studies also showed evidence of partial stomatal opening at night, indicating the importance of transpiration for ET_{night} (Li et al., 2023b; Padron et al., 2020; Yu et al., 2019; Zeppel et al., 2014). Moreover, contrary to the fact that elevated CO_2 reduces daytime stomatal conductance, nocturnal stomatal conductance might increase with elevated CO_2 in the future due to the increased sap flow, potentially increasing water loss and susceptibility to drought (Zeppel et al., 2012). While transgenerational effects of elevated CO_2 were found to improve daytime plant water use efficiency under drought stress (Li et al., 2017), there is still a clear lack of evidence how elevated CO_2 will affect nocturnal evapotranspiration.

4.2. *Environmental variables influencing NRW input and ET_{night} losses*

Chen et al. (2013) suggested that meteorological conditions for dew formation differed significantly among various studies, and thus resulted in different NRW inputs. In our study, ΔT_{air} was indeed the main driver of NRW gains (Fig. 7a), because any change in air temperature (ΔT_{air}) during NRW input events indicates the strength of radiative cooling (Li et al., 2023b; Monteith, 1957). Moreover, with a specific condensation rate, longer duration of NRW events would induce higher NRW gains (Ritter et al., 2019), supported by our RF model with duration as the second most important driver of NRW gains (Fig. 7a). Wind speed was one of the important drivers of NRW gains as well (Fig. 7a), most likely because dew and radiation fog occur on clear and calm nights with a stable stratified nocturnal boundary layer (Garratt and Segal, 1988); as dew condensation is positively related with the wind speed gradient (Monteith, 1957). Despite the fact that dew occurs when surfaces cool below dew point temperature, radiative cooling and condensation heat release induce fluctuations of ΔT (Monteith, 1957). Therefore, ΔT was not directly linked to NRW gain, but was nevertheless recognized as the fourth important driver of NRW inputs (Fig. 7a). Although NRW occurred under high-humidity and saturated conditions (Monteith, 1957), VPD and RH were less important to explain NRW inputs (Fig. 7a), probably due to the general higher RH and lower VPD with the occurrence of NRW. Thus, depending how these meteorological conditions change in the future, e.g., under climate change or with different management practises for grassland use, the relevance of NRW inputs might increase, although the overall NRW input is very low.

According to the Penman-Monteith equation, evaporation is correlated with the vapor pressure gradient between saturated vapor pressure

and atmospheric vapor pressure, and thus the difference between air temperature and dew-point temperature (Widmoser, 2009). Therefore, ΔT was recognized as the most important driver of ET_{night} in our study during the absence of solar irradiation (Fig. 7b). Soil moisture is typically the main water source of ET_{night} and can thus promote ET_{night} (Padron et al., 2020). Indeed, SWC was recognized as the second most important driver of ET_{night} losses across our nine sites (Fig. 7b). In contrast, Groh et al. (2019) found only a weak positive correlation between SWC and ET_{night}. Nevertheless, although the average difference in SWC between NRW inputs and ET_{night} losses was only 2.99 ± 0.14 m^3 m^{-3}, SWC was not only an important variable for ET_{night}, but also for the combined NRW–ET_{night} events (Fig. 7c). In contrast to the occurrence of dew and radiation fog on clear and calm nights, ET_{night} events were observed under conditions with much stronger wind speed (Table 3), reflecting turbulent conditions strongly promoting ET_{night} (Whiteman et al., 2007). Independent of the dominant process of ET_{night}, transpiration or evaporation, water loss during the night will further increase in the future, since not only soil water supply, but also increasing temperatures and VPD, as reported globally (Qiao et al., 2023), will increase ET_{night}, with potentially negative effects on grassland performance.

ΔT showed negative values during NRW inputs, but positive values during nights ET_{night} losses (Monteith, 1957), thus ΔT was recognized as the most important driver for the grassland water changes during combined NRW–ET_{night} events (Fig. 7c). SWC was slightly higher during NRW input events compared to that during ET_{night} events (Table 3). Thus, SWC was not directly linked to NRW inputs, but was the main driver of ET_{night} events (Padron et al., 2020), and thus recognized as the second most important driver for combined NRW–ET_{night} events (Fig. 7c). RH and U are important conditions for distinguishing NRW and ET_{night} events (Li et al., 2021; Monteith, 1957), also recognized as third and fourth important drivers of water change during combined NRW–ET_{night} events. The accuracy of using these important variables to predict nocturnal water gain and/or loss still needs to be tested for different locations and ecosystem types to show their applicability for simulating NRW gains or ET_{night} water losses.

4.3. *NRW inputs and ET_{night} affected net ecosystem exchange in the early morning hours*

The NEE in the first two hours after sunrise was significantly reduced following a NRW input event compared to the morning hours following an ET_{night} event (Fig. 8a). Compared to ET_{night} events, higher CO_2 gradients from air towards the canopy after NRW events might intensify plant carbon uptake (Ben-Asher et al., 2010), and thus lower NEE in the morning hours at same levels of PPFD as after ET_{night} events (Fig. 8c). Besides, the clogging of stomata by NRW droplets might suppress CO_2 emissions, and lower NEE after NRW input nights (Gerlein-Safdi et al., 2018a; Gerlein-Safdi et al., 2018b; Oliveira et al., 2021). Despite a small amount of water compared to rainfall, NRW plays a key role in maintaining ecosystem functionality by lowering transpiration thanks to low leaf-to-air vapor pressure gradient, promoting photosynthesis attributed to high air-to-canopy CO_2 gradient, and providing additional water sources, especially during dry spells. In California redwood forest, fog was found to contribute 34 % of hydrological inputs, and provide up to 66 % of plant water for understory plants (Dawson and Goldsmith, 2018). Photosynthetic rates during leaf wetting and drying processes were found to vary across many species, and species that hold more water on the surface tend to have a higher net photosynthesis (Aparecido et al., 2017). Harvesting dew water was found to be sufficient for irrigating tree seedling and mitigating tree mortality in dry regions (Tomaszkiewicz et al., 2017). In this study, we only focused on the influence of NRW on NEE in early morning hours. The diel and seasonal influence of NRW on NEE was not investigated. It still needs further methods to explore the long-term meaning of NRW on ecosystem NEE.

Early morning NEE increased significantly with air temperature following an ET_{night} event, while the relationship with PPFD was not significant, indicating an increased risk of climate change on ET_{night}. Schoppach et al. (2020) reported that increased night transpiration can lead to wheat yield reduction, whereas increased predawn transpiration can improve yield. However, Resco de Dios et al. (2015) stated that circadian controls can reduce water loss and foster carbon uptake. Other research indicated the variable response of night-time transpiration to increasing VPD (Tamang et al., 2019). Therefore, the effect of night-time evapotranspiration on NEE is influenced by the variability of nocturnal (e.g., night or predawn) environmental conditions.

5. Conclusions

Our study showed that water gains and losses of NRW inputs and ET_{night} did not change along the elevation gradient, but was affected by terrain. Sites with higher occurrence frequency and gains of NRW inputs tended to have lower occurrence frequency and water loss of ET_{night}. The most important drivers of NRW gains were air temperature changes, duration of NRW, and wind speed, while the temperature difference between surface and dew-point temperatures, soil moisture, and wind speed were the most important drivers of ET_{night} water loss. Soil moisture was the main source of ET_{night}, and was thus one of the important indicators of predicting NRW–ET_{night} events. These environmental variables used for simulating nocturnal grassland water budgets still need to be tested at global scales and for different ecosystem types. Grassland NEE did not profit from NRW gains within two hours after sunrise. Thus, relevance of NRW inputs in terms of water amounts for temperate grasslands was low, while increasing occurrence and higher rates of ET_{night} will pose additional risks to grasslands in the future.

Author contribution

Yafei Li: Participating in the experiment design; drafting and revising the manuscript.

Andreas Riedl: Leading and maintaining the experiment; drafting and revising the manuscript.

Werner Eugster: Participating in the experiment design; commenting and revising early stages of the manuscript (passed away on 23 May 2022 before the final submission of this study).

Nina Buchman: Participating in the experiment design; commenting and revising the manuscript.

CRediT authorship contribution statement

Yafei Li: Writing – review & editing, Writing – original draft, Visualization, Validation, Methodology, Investigation, Formal analysis, Data curation, Conceptualization. **Andreas Riedl:** Writing – review & editing, Writing – original draft, Visualization, Validation, Methodology, Investigation, Formal analysis, Data curation, Conceptualization. **Nina Buchmann:** Writing – review & editing, Supervision, Funding acquisition, Conceptualization. **Werner Eugster:** Writing – review & editing, Supervision, Funding acquisition, Conceptualization.

Declaration of competing interest

The authors declare that they have no known competing financial interests or personal relationships that could have appeared to influence the work reported in this paper.

Acknowledgement

We thank Paul Linwood, Markus Staudinger, Philip Meier, Thomas Baur, and Patrick Flütsch, ETH Zurich, for their technical support. We thank Dr. Iris Feigenwinter and Dr. Lukas Hörtnagl, ETH Zurich, for the quality check of EC and meteorological data. We thank the station managers and station staff at all study sites. We thank WSL for the access

of meteorological data at their stations.

Appendix A. Supplementary data

Supplementary data to this article can be found online at https://doi.org/10.1016/j.jhydrol.2025.134632.

Data availability

Data were deposited at the ETH Zurich research collection at https://doi.org/10.5905/ethz-1002-22985 (Riedl, 2025).

References

Agam, N., Berliner, P.R., 2006. Dew formation and water vapor adsorption in semi-arid environments – a review. J. Arid Environ. 65 (4), 572–590. https://doi.org/10.1016/j.jaridenv.2005.09.004.

Aguirre-Gutiérrez, C.A., Holwerda, F., Goldsmith, G.R., Delgado, J., Yepez, E., Carbajal, N., Escoto-Rodríguez, M., Arredondo, J.T., 2019. The importance of dew in the water balance of a continental semiarid grassland. J. Arid Environ. 168, 26–35. https://doi.org/10.1016/j.jaridenv.2019.05.003.

Alduchov, O.A., Eskridge, R.E., 1996. Improved magnus form approximation of saturation vapor pressure. J. Appl. Meteorol. Clim. 35 (4), 601–609. https://doi.org/10.1175/1520-0450(1996)035<0601:IMFAOS>2.0.CO;2.

Allan, R.P., Arias, P.A., Barlow, M., Cerezo-Mota, R., Cherchi, A., Gan, T., Gergis, J., Jiang, D., Khan, A., Mba, W.P., Rosenfeld, D., Tierney, J., Zolina, O., 2021. Water cycle changes, Climate Change 2021: The Physical science basis. Contribution of Working Group I to the sixth assessment report of the intergovernmental panel on climate change. The Intergovernmental Panel on Climate Change (IPCC) available at https://www.ipcc.ch/report/ar6/wg1/(last access 2 December 2021).

Aparecido, L.M.T., Miller, G.R., Cahill, A.T., Moore, G.W., 2017. Leaf surface traits and water storage retention affect photosynthetic responses to leaf surface wetness among wet tropical forest and semiarid savanna plants. Tree Physiol. 37 (10), 1285–1300. https://doi.org/10.1093/treephys/tpx092.

Aubinet, M., Vesala, T., Papale, D., 2012. Eddy Covariance: A Practical Guide to Measurement and Data Analysis. Springer, Dordrecht, p. 438.

Baldocchi, D., 2014. Measuring fluxes of trace gases and energy between ecosystems and the atmosphere – the state and future of the eddy covariance method. Glob. Chang. Biol. 20 (12), 3600–3609. https://doi.org/10.1111/gcb.12649.

Ben-Asher, J., Alpert, P., Ben-Zvi, A., 2010. Dew is a major factor affecting vegetation water use efficiency rather than a source of water in the eastern Mediterranean area. Water Resour. Res. 46, W10532. https://doi.org/10.1029/2008WR007484.

Boergens, E., Güntner, A., Dobslaw, H., Dahle, C., 2020. Quantifying the central European droughts in 2018 and 2019 with GRACE follow-on. Geophys. Res. Lett. 47 (14), e2020GL087285. https://doi.org/10.1029/2020GL087285.

Boucher, J.F., Munson, A.D., Bernier, P.Y., 1995. Foliar absorption of dew influences shoot water potential and root-growth in pinus-strobus seedlings. Tree Physiol. 15 (12), 819–823. https://doi.org/10.1093/treephys/15.12.819.

Breiman, L., 2001. Random forests. Mach. Learn. 45 (1), 5–32. https://doi.org/10.1023/A:1010933404324.

Caird, M.A., Richards, J.H., Hsiao, T.C., 2007. Significant transpirational water loss occurs throughout the night in field-grown tomato. Funct. Plant Biol. 34 (3), 172–177. https://doi.org/10.1071/FP06264.

Chen, L., Meissner, R., Zhang, Y., Xiao, H., 2013. Studies on dew formation and its meteorological factors. J. Food Agric. Environ. 11 (2), 1063–1068. Available at: https://www.wflpublisher.com/Abstract/4506 (last access 11 November 2023).

Christman, M.A., Donovan, L.A., Richards, J.H., 2009. Magnitude of nighttime transpiration does not affect plant growth or nutrition in well-watered Arabidopsis. Physiol. Plant. 136 (3), 264–273. https://doi.org/10.1111/j.1399-3054.2009.01216.x.

Dawson, T.E., Goldsmith, G.R., 2018. The value of wet leaves. New Phytol. 219 (4), 1156–1169. https://doi.org/10.1111/nph.15307.

Eugster, W., Burkard, R., Holwerda, F., Scatena, F.N., Bruijnzeel, L.A., 2006. Characteristics of fog and fogwater fluxes in a Puerto rican elfin cloud forest. Agric. For. Meteorol. 139 (3), 288–306. https://doi.org/10.1016/j.agrformet.2006.07.008.

Eugster, W., Siegrist, F., 2000. The influence of nocturnal CO_2 advection on CO_2 flux measurements. Basic Appl. Ecol. 1 (2), 177–188. https://doi.org/10.1078/1439-1791-00028.

Fatichi, S., Zeeman, M.J., Fuhrer, J., Burlando, P., 2014. Ecohydrological effects of management on subalpine grasslands: from local to catchment scale. Water Resour. Res. 50 (1), 148–164. https://doi.org/10.1002/2013WR014535.

Feigenwinter, I., Hörtnagl, L., Zeeman, M.J., Eugster, W., Fuchs, K., Merbold, L., Buchmann, N., 2023. Large inter-annual variation in carbon sink strength of a permanent grassland over 16 years: Impacts of management practices and climate. Agric. For. Meteorol. 340, 109613. https://doi.org/10.1016/j.agrformet.2023.109613.

Fuchs, K., Hörtnagl, L., Buchmann, N., Eugster, W., Snow, V., Merbold, L., 2018. Management matters: testing a mitigation strategy for nitrous oxide emissions using legumes on intensively managed grassland. Biogeosciences 15 (18), 5519–5543. https://doi.org/10.5194/bg-15-5519-2018.

Garratt, J.R., Segal, M., 1988. On the contribution of atmospheric moisture to dew formation. Bound.-Lay. Meteorol. 45 (3), 209–236. https://doi.org/10.1007/bf01066671.

Gerlein-Safdi, C., Gauthier, P.P.G., Caylor, K.K., 2018a. Dew-induced transpiration suppression impacts the water and isotope balances of Colocasia leaves. Oecologia 187 (4), 1041–1051. https://doi.org/10.1007/s00442-018-4199-y.

Gerlein-Safdi, C., Koohafkan, M.C., Chung, M., Rockwell, F.E., Thompson, S., Caylor, K. K., 2018b. Dew deposition suppresses transpiration and carbon uptake in leaves. Agric. For. Meteorol. 259, 305–316. https://doi.org/10.1016/j.agrformet.2018.05.015.

Goldsmith, G.R., 2013. Changing directions: the atmosphere-plant-soil continuum. New Phytol. 199 (1), 4–6. https://doi.org/10.1111/nph.12332.

Groh, J., Putz, T., Gerke, H.H., Vanderborght, J., Vereecken, H., 2019. Quantification and prediction of nighttime evapotranspiration for two distinct grassland ecosystems. Water Resour. Res. 55 (4), 2961–2975. https://doi.org/10.1029/2018wr024072.

Groh, J., Slawitsch, V., Herndl, M., Graf, A., Vereecken, H., Pütz, T., 2018. Determining dew and hoar frost formation for a low mountain range and alpine grassland site by weighable lysimeter. J. Hydrol. 563, 372–381. https://doi.org/10.1016/j.jhydrol.2018.06.009.

Guo, X., Xiao, J., Zha, T., Shang, G., Liu, P., Jin, C., Zhang, Y., 2023. Dynamics and biophysical controls of nocturnal water loss in a winter wheat-summer maize rotation cropland: a multi-temporal scale analysis. Agric. For. Meteorol. 342, 109701. https://doi.org/10.1016/j.agrformet.2023.109701.

Han, Q., Wang, T., Wang, L., Smettem, K., Mai, M., Chen, X., 2021. Comparison of nighttime with daytime evapotranspiration responses to environmental controls across temporal scales along a climate gradient. Water Resour. Res. 57 (7), e2021WR029638. https://doi.org/10.1029/2021WR029638.

Jacobs, A.F.G., Heusinkveld, B.G., Berkowicz, S.M., 2002. A simple model for potential dewfall in an arid region. Atmos. Res. 64 (1–4), 285–295. https://doi.org/10.1016/S0169-8095(02)00099-6.

Jacobs, A.F.G., Heusinkveld, B.G., Kruit, R.J.W., Berkowicz, S.M., 2006. Contribution of dew to the water budget of a grassland area in the Netherlands. Water Resour. Res. 42 (3), W03415. https://doi.org/10.1029/2005WR004055.

Jia, Z., Wang, Z., Wang, H., 2019. Characteristics of dew formation in the semi-arid loess plateau of central Shaanxi Province, China. Water. https://doi.org/10.3390/w11010126.

Li, Y., Aemisegger, F., Riedl, A., Buchmann, N., Eugster, W., 2021. The role of dew and radiation fog inputs in the local water cycling of a temperate grassland during dry spells in central Europe. Hydrol. Earth Syst. Sci. 25 (5), 2617–2648. https://doi.org/10.5194/hess-25-2617-2021.

Li, Y., Eugster, W., Riedl, A., Lehmann, M.M., Aemisegger, F., Buchmann, N., 2023a. Dew benefits on alpine grasslands are cancelled out by combined heatwave and drought stress. Front. Plant Sci. 14. https://doi.org/10.3389/fpls.2023.1136037.

Li, Y., Li, X., Yu, J., Liu, F., 2017. Effect of the transgenerational exposure to elevated CO2 on the drought response of winter wheat: Stomatal control and water use efficiency. Environ. Exp. Bot. 136, 78–84. https://doi.org/10.1016/j.envexpbot.2017.01.006.

Li, Y., Riedl, A., Eugster, W., Buchmann, N., Cernusak, L.A., Lehmann, M.M., Werner, R. A., Aemisegger, F., 2023b. The role of radiative cooling and leaf wetting in air–leaf water exchange during dew and radiation fog events in a temperate grassland. Agric. For. Meteorol. 328, 109256. https://doi.org/10.1016/j.agrformet.2022.109256.

LI-COR: Eddy covariance processing software, Version 7.0.4 [Software], LI-COR, Inc, available at: https://www.licor.com/env/products/eddy_covariance/software.html (last access: 19 Nov 2025), 2019.

Limm, E.B., Simonin, K.A., Bothman, A.G., Dawson, T.E., 2009. Foliar water uptake: a common water acquisition strategy for plants of the redwood forest. Oecologia 161 (3), 449–459. https://doi.org/10.1007/s00442-009-1400-3.

López, A., Molina-Aiz, F.D., Valera, D.L., Peña, A., 2012. Determining the emissivity of the leaves of nine horticultural crops by means of infrared thermography. Sci. Hortic. 137, 49–58. https://doi.org/10.1016/j.scienta.2012.01.022.

Malek, E., 1992. Night-time evapotranspiration vs. daytime and 24h evapotranspiration. J. Hydrol. 138 (1), 119–129. https://doi.org/10.1016/0022-1694(92)90159-S.

Malek, E., McCurdy, G., Giles, B., 1999. Dew contribution to the annual water balances in semi-arid desert valleys. J. Arid Environ. 42 (2), 71–80. https://doi.org/10.1006/jare.1999.0506.

MeteoSwiss, 2025. Heatwaves, droughts, cold and snowfall. https://www.meteoswiss.admin.ch/climate/climate-change/heatwaves-droughts-cold-and-snowfall.html.

Minnis, P., Mayor, S., Smith, W.L., Young, D.F., 1997. Asymmetry in the diurnal variation of surface albedo. IEEE Trans. Geosci. Remote Sens. 35 (4), 879–890. https://doi.org/10.1109/36.602530.

Misson, L., Lunden, M., McKay, M., Goldstein, A.H., 2005. Atmospheric aerosol light scattering and surface wetness influence the diurnal pattern of net ecosystem exchange in a semi-arid ponderosa pine plantation. Agric. For. Meteorol. 129 (1), 69–83. https://doi.org/10.1016/j.agrformet.2004.11.008.

Moene, A.F., van Dam, J.C., 2014. Transport in the Atmosphere-Vegetation-Soil Continuum. Cambridge University Press, Cambridge, 10.1017/CBO9781139043137.

Monteith, J.L., 1957. Dew. Quart. J. Royal Meteorol. Soc. 83 (357), 322–341. https://doi.org/10.1002/qj.49708335706.

Munné-Bosch, S., Alegre, L., 1999. Role of dew on the recovery of water-stressed Melissa officinalis L. plants. J. Plant Physiol. 154 (5), 759–766. https://doi.org/10.1016/S0176-1617(99)80255-7.

Oliveira, B.R.F., Schaller, C., Keizer, J.J., Foken, T., 2021. Estimating immediate post-fire carbon fluxes using the eddy-covariance technique. Biogeosciences 18 (1), 285–302. https://doi.org/10.5194/bg-18-285-2021.

Padron, R.S., Gudmundsson, L., Michel, D., Seneviratne, S.I., 2020. Terrestrial water loss at night: global relevance from observations and climate models. Hydrol. Earth Syst. Sci. 24 (2), 793–807. https://doi.org/10.5194/hess-24-793-2020.

Pastorello, G., Trotta, C., Canfora, E., Chu, H., Christianson, D., Cheah, Y.-W., Poindexter, C., Chen, J., Elbashandy, A., Humphrey, M., Isaac, P., Polidori, D., Reichstein, M., Ribeca, A., van Ingen, C., Vuichard, N., Zhang, L., Amiro, B., Ammann, C., Arain, M.A., Ardö, J., Arkebauer, T., Arndt, S.K., Arriga, N., Aubinet, M., Aurela, M., Baldocchi, D., Barr, A., Beamesderfer, E., Marchesini, L.B., Bergeron, O., Beringer, J., Bernhofer, C., Berveiller, D., Billesbach, D., Black, T.A., Blanken, P.D., Bohrer, G., Boike, J., Bolstad, P.V., Bonal, D., Bonnefond, J.-M., Bowling, D.R., Bracho, R., Brodeur, J., Brümmer, C., Buchmann, N., Burban, B., Burns, S.P., Buysse, P., Cale, P., Cavagna, M., Cellier, P., Chen, S., Chini, I., Christensen, T.R., Cleverly, J., Collalti, A., Consalvo, C., Cook, B.D., Cook, D., Coursolle, C., Cremonese, E., Curtis, P.S., D'Andrea, E., da Rocha, H., Dai, X., Davis, K.J., Cinti, B.D., Grandcourt, A.D., Ligne, A.D., De Oliveira, R.C., Delpierre, N., Desai, A.R., Di Bella, C.M., Tommasi, P.D., Dolman, H., Domingo, F., Dong, G., Dore, S., Duce, P., Dufrêne, E., Dunn, A., Dušek, J., Eamus, D., Eichelmann, U., ElKhidir, H.A.M., Eugster, W., Ewenz, C.M., Ewers, B., Famulari, D., Fares, S., Feigenwinter, I., Feitz, A., Fensholt, R., Filippa, G., Fischer, M., Frank, J., Galvagno, M., Gharun, M., Gianelle, D., Gielen, B., Gioli, B., Gitelson, A., Goded, I., Goeckede, M., Goldstein, A.H., Gough, C.M., Goulden, M.L., Graf, A., Griebel, A., Gruening, C., Grünwald, T., Hammerle, A., Han, S., Han, X., Hansen, B.U., Hanson, C., Hatakka, J., He, Y., Hehn, M., Heinesch, B., Hinko-Najera, N., Hörtnagl, L., Hutley, L., Ibrom, A., Ikawa, H., Jackowicz-Korczynski, M., Janouš, D., Jans, W., Jassal, R., Jiang, S., Kato, T., Khomik, M., Klatt, J., Knohl, A., Knox, S., Kobayashi, H., Koerber, G., Kolle, O., Kosugi, Y., Kotani, A., Kowalski, A., Kruijt, B., Kurbatova, J., Kutsch, W.L., Kwon, H., Launiainen, S., Laurila, T., Law, B., Leuning, R., Li, Y., Liddell, M., Limousin, J.-M., Lion, M., Liska, A.J., Lohila, A., López-Ballesteros, A., López-Blanco, E., Loubet, B., Loustau, D., Lucas-Moffat, A., Lüers, J., Ma, S., Macfarlane, C., Magliulo, V., Maier, R., Mammarella, I., Manca, G., Marcolla, B., Margolis, H.A., Marras, S., Massman, W., Mastepanov, M., Matamala, R., Matthes, J.H., Mazzenga, F., McCaughey, H., McHugh, I., McMillan, A.M.S., Merbold, L., Meyer, W., Meyers, T., Miller, S.D., Minerbi, S., Moderow, U., Monson, R.K., Montagnani, L., Moore, C.E., Moors, E., Moreaux, V., Moureaux, C., Munger, J.W., Nakai, T., Neirynck, J., Nesic, Z., Nicolini, G., Noormets, A., Northwood, M., Nosetto, M., Nouvellon, Y., Novick, K., Oechel, W., Olesen, J.E., Ourcival, J.-M., Papuga, S.A., Parmentier, F.-J., Paul-Limoges, E., Pavelka, M., Peichl, M., Pendall, E., Phillips, R.P., Pilegaard, K., Pirk, N., Posse, G., Powell, T., Prasse, H., Prober, S.M., Rambal, S., Rannik, Ü., Raz-Yaseef, N., Rebmann, C., Reed, D., Dios, V.R.D., Restrepo-Coupe, N., Reverter, B.R., Roland, M., Sabbatini, S., Sachs, T., Saleska, S.R., Sánchez-Cañete, E.P., Sanchez-Mejia, Z.M., Schmid, H.P., Schmidt, M., Schneider, K., Schrader, F., Schroder, I., Scott, R.L., Sedlák, P., Serrano-Ortíz, P., Shao, C., Shi, P., Shironya, I., Siebicke, L., Šigut, L., Silberstein, R., Sirca, C., Spano, D., Steinbrecher, R., Stevens, R.M., Sturtevant, C., Suyker, A., Tagesson, T., Takanashi, S., Tang, Y., Tapper, N., Thom, J., Tomassucci, M., Tuovinen, J.-P., Urbanski, S., Valentini, R., van der Molen, M., van Gorsel, E., van Huissteden, K., Varlagin, A., Verfaillie, J., Vesala, T., Vincke, C., Vitale, D., Vygodskaya, N., Walker, J.P., Walter-Shea, E., Wang, H., Weber, R., Westermann, S., Wille, C., Wofsy, S., Wohlfahrt, G., Wolf, S., Woodgate, W., Li, Y., Zampedri, R., Zhang, J., Zhou, G., Zona, D., Agarwal, D., Biraud, S., Torn, M., Papale, D., 2020. The FLUXNET2015 dataset and the ONEFlux processing pipeline for eddy covariance data. Sci. Data 7 (1), 225. https://doi.org/10.1038/s41597-020-0534-3.

Pedregosa, F., 2011. Scikit-learn: machine learning in Python. J. Mach. Learn. Res. 12, 2825.

Qiao, L., Zuo, Z., Zhang, R., Piao, S., Xiao, D., Zhang, K., 2023. Soil moisture–atmosphere coupling accelerates global warming. Nat. Commun. 14 (1), 4908. https://doi.org/10.1038/s41467-023-40641-y.

Resco de Dios, V., Chowdhury, F.I., Granda, E., Yao, Y., Tissue, D.T., 2019. Assessing the potential functions of nocturnal stomatal conductance in C3 and C4 plants. New Phytol. 223 (4), 1696–1706. https://doi.org/10.1111/nph.15881.

Resco de Dios, V., Roy, J., Ferrio, J.P., Alday, J.G., Landais, D., Milcu, A., Gessler, A., 2015. Processes driving nocturnal transpiration and implications for estimating land evapotranspiration. Sci. Rep.-UK 5 (1), 10975. https://doi.org/10.1038/srep10975.

Riedl, A., Li, Y., Eugster, J., Buchmann, N., Eugster, W., 2022. Technical note: high-accuracy weighing micro-lysimeter system for long-term measurements of non-rainfall water inputs to grasslands. Hydrol. Earth Syst. Sci. 2021, 1–34. https://doi.org/10.5194/hess-26-91-2022.

Ritter, F., Berkelhammer, M., Beysens, D., 2019. Dew frequency across the US from a network of in situ radiometers. Hydrol. Earth Syst. Sci. 23 (2), 1179–1197. https://doi.org/10.5194/hess-23-1179-2019.

Rogger, J., Hörtnagl, L., Buchmann, N., Eugster, W., 2022. Carbon dioxide fluxes of a mountain grassland: drivers, anomalies and annual budgets. Agric. For. Meteorol. 314, 108801. https://doi.org/10.1016/j.agrformet.2021.108801.

Scherrer, S.C., Appenzeller, C., 2014. Fog and low stratus over the Swiss Plateau – a climatological study. Int. J. Climatol. 34 (3), 678–686. https://doi.org/10.1002/joc.3714.

Schoppach, R., Sinclair, T.R. and Sadok, W., 2020. Sleep tight and wake-up early: nocturnal transpiration traits to increase wheat drought tolerance in a Mediterranean environment. (1445-4416 (Electronic)).

Seabold, S., Perktold, J., 2010. Statsmodels: Econometric and statistical modeling with python. In: Proceedings of the 9th Python in Science Conference. Austin, TX, pp. 10–25080.

Simonin, K.A., Santiago, L.S., Dawson, T.E., 2009. Fog interception by Sequoia sempervirens (D. Don) crowns decouples physiology from soil water deficit. Plant Cell Environ. 32 (7), 882–892. https://doi.org/10.1111/j.1365-3040.2009.01967.x.

Stoll, S., Hendricks Franssen, H.-J., Bárdossy, A., Kinzelbach, W., 2013. On the relationship between atmospheric circulation patterns, recharge and soil moisture dynamics in Switzerland. J. Hydrol. 502, 1–9. https://doi.org/10.1016/j.jhydrol.2013.08.017.

Strobl, C., Boulesteix, A.-L., Zeileis, A., Hothorn, T., 2007. Bias in random forest variable importance measures: Illustrations, sources and a solution. BMC Bioinf. 8 (1), 25. https://doi.org/10.1186/1471-2105-8-25.

Tamang, B.G., Schoppach, R., Monnens, D., Steffenson, B.J., Anderson, J.A., Sadok, W., 2019. Variability in temperature-independent transpiration responses to evaporative demand correlate with nighttime water use and its circadian control across diverse wheat populations. Planta 250 (1), 115–127. https://doi.org/10.1007/s00425-019-03151-0.

Tomaszkiewicz, M., Abou Najm, M., Zurayk, R., El-Fadel, M., 2017. Dew as an adaptation measure to meet water demand in agriculture and reforestation. Agric. For. Meteorol. 232, 411–421. https://doi.org/10.1016/j.agrformet.2016.09.009.

Ucles, O., Villagarcia, L., Canton, Y., Domingo, F., 2013. Microlysimeter station for long term non-rainfall water input and evaporation studies. Agric. For. Meteorol. 182, 13–20. https://doi.org/10.1016/j.agrformet.2013.07.017.

Whiteman, C.D., De Wekker, S.F.J., Haiden, T., 2007. Effect of dewfall and frostfall on nighttime cooling in a small, closed basin. J Appl Meteorol Clim 46 (1), 3–13. https://doi.org/10.1175/Jam2453.1.

Widmoser, P., 2009. A discussion on and alternative to the Penman–Monteith equation. Agric. Water. Manag. 96 (4), 711–721. https://doi.org/10.1016/j.agwat.2008.10.003.

Xiao, H., Meissner, R., Seeger, J., Rupp, H., Borg, H., 2009. Effect of vegetation type and growth stage on dewfall, determined with high precision weighing lysimeters at a site in northern Germany. J. Hydrol. 377 (1), 43–49. https://doi.org/10.1016/j.jhydrol.2009.08.006.

Yokoyama, G., Yasutake, D., Wang, W., Wu, Y., Feng, J., Dong, L., Kimura, K., Marui, A., Hirota, T., Kitano, M., Mori, M., 2021. Limiting factor of dew formation changes seasonally in a semiarid crop field of northwest China. Agric. For. Meteorol. 311, 108705. https://doi.org/10.1016/j.agrformet.2021.108705.

Yu, K., Goldsmith, G.R., Wang, Y., Anderegg, W.R.L., 2019. Phylogenetic and biogeographic controls of plant nighttime stomatal conductance. New Phytol. 222 (4), 1778–1788. https://doi.org/10.1111/nph.15755.

Zeppel, M.J.B., Lewis, J.D., Chaszar, B., Smith, R.A., Medlyn, B.E., Huxman, T.E., Tissue, D.T., 2012. Nocturnal stomatal conductance responses to rising [CO2], temperature and drought. New Phytol. 193 (4), 929–938. https://doi.org/10.1111/j.1469-8137.2011.03993.x.

Zeppel, M.J.B., Lewis, J.D., Phillips, N.G., Tissue, D.T., 2014. Consequences of nocturnal water loss: a synthesis of regulating factors and implications for capacitance, embolism and use in models. Tree Physiol. 34 (10), 1047–1055. https://doi.org/10.1093/treephys/tpu089.

Zhang, J., Zhang, Y.-M., Downing, A., Cheng, J.-H., Zhou, X.-B., Zhang, B.-C., 2009. The influence of biological soil crusts on dew deposition in Gurbantunggut Desert, Northwestern China. J. Hydrol. 379 (3–4), 220–228. https://doi.org/10.1016/j.jhydrol.2009.09.053.